ICEMG 2023-XXXXX

Structural analysis of the rotor core of a switched reluctance motor in both constant torque and constant power regions

Nasrin Majlesi[1], Sayed Morteza Saghaian Nejad[2], Amir Rashidi[3]

[1]Master Student, Isfahan University of Technology, Isfahan, Iran; n.majlesi@ec.iut.ac.ir

[2]Professor, Isfahan University of Technology/Electrical and Computer Engineering Department, Isfahan, Iran; saghaian@iut.ac.ir

[3]Hakim Sabzevari University/Electrical and Computer Engineering Department, Sabzevar, Iran; 315.amir@gmail.com

Abstract

Because of robust rotor structure, switched reluctance motor (SRM) can be a good candidate for high-speed applications. Due to high centrifugal forces at high-speed, structural analysis of the rotor core in an indispensable part of the design. In this paper, a 4kW-3000rpm SRM is considered. The maximum speed of the case-study motor is 7000rpm. The aim is structural and failure analysis of the rotor core in both constant torque and constant power regions. Deformations and stresses experienced by the rotor core for various operating modes are calculated by finite element method and velocity-deformation and velocity- von-Mises stress curves are presented. The aim is feasibility study of using of SRM for high-speed applications and providing some design guidelines for rigid design of the rotor core.

Keywords: Switched reluctance motor, High-speed, Structural analysis, von-Mises stress, Deformation

Introduction

Compared to the permanent magnet and induction motors, switched reluctance motors (SRMs) have a simple, low-cost, and robust construction. The stator core of SRM has a salient pole structure with concentrated coils on each pole, while the rotor case has a salient pole structure without windings or permanent magnets [1]. This rotor structure enables reliable operation at high speeds and high temperatures but also brings many challenges, such as high torque ripples, acoustic noise, and vibration [2-4]. The robustness of SRM is significant for many applications, which makes rotor structural analysis an important step of the design process.

Centrifugal forces exist in the rotating parts of the motor. These forces create radial and tangential stresses, which cause deformations inside the rotor core. Because the centrifugal force is proportional to the rotor speed squared, the higher rotational speed causes higher stresses [5]. Stresses are concentrated around any sharp corners of the rotor. The highest value of tangential stress occurs around the shaft. At high speeds, the vibrations and natural frequencies require careful attention as they affect acoustic noise, bearing losses and the risk of failure [6, 7].

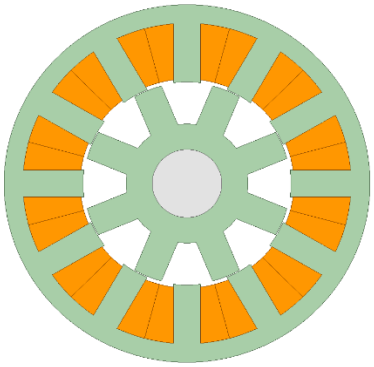

Figure 1. The case-study motor structure

In electric motors, large stresses are often generated at the stator yoke by shrink fitting of stator housings. In this case, the permeability decreases, whereas the core loss increases with the compressive stress [8]. There is a relationship between the power losses caused by the mechanical processing of the core sheets and the stress and deformation caused by this process. Therefore, due to the dependence of iron losses on stress and strain, an accurate multi-physics analysis of the motor is needed [9]. The rotor, which is the only rotating part in a motor, is likely to experience significant stresses and deformations.

During low-speed operation, the magnetic forces experienced by the rotor are greater than the centrifugal forces. Hence, most of the stresses and deformations experienced at low speeds are mainly due to magnetic forces. At higher speeds, centrifugal forces become the only cause of deformations on the rotating body resulting structural failure [10].

In [11] radial forces are applied to the stator core for static structural analysis using 3D FEA to compare total deformation with a corresponding induction motor. From the static structural analysis, it can be concluded that if the motor is designed with a 12/8 structure instead of 6/4 the maximum total deformation can be reduced to 1.26%.

This paper presents a structural analysis of a 4kW-3000rpm case-study SRM in a wide operating speed range. Deformations and stresses are calculated for several operating points in both constant torque and constant power regions by the finite element method. The

aim is to determine stresses and deformations in the rotor core and identify the causes of failure on the proposed motor to provide some guidelines for designing a robust rotor core structure. The ANSYS Maxwell software is used for electromagnetic analysis, and the ANSYS Transient Structural package is used for deformation calculations.

Case-study motor

The stator and rotor pole combination of the case-study motor is 12/8. It has a three-phase winding which is fed by an asymmetric bridge converter. The motor structure is shown in Figure 1. Table 1 shows the geometrical dimensions and specification of the case-study motor. The rated output power of the motor at the base speed is 4kW.

Table 1. Specifications of the case-study motor

Parameter	Value
Rated output power	4kW
Rated speed	3000rpm
Rated torque	12.7Nm
Maximum speed	7000rpm
DC link voltage	300V
Stator bore diameter	84mm
Outer stator diameter	140mm
Stack length	100mm
Electric steel grade	M270-35A
Number of stator poles	12
Number of rotor poles	8
Number of phases	3

Rigidity analysis

Structural analysis of an electric motor is the study of deformations and stresses experienced by all motor parts. Mechanical properties of the materials used in the motor structure such as Young's modulus are used in the elasticity equation to evaluate the strength of the structure and the maximum pressure that the structure can withstand [12]. Transient structural analysis is the process of calculating and determining the effects of loads and internal forces that are a function of time on a structure. In this work, we considered magnetic force and centrifugal force as the sources that cause deformations and stresses on the rotor. The mechanical stresses limit the maximum circumferential speed and accordingly the outer diameter of the rotor, the bore volume, and the power of the electric motor. Thus, the calculation of the mechanical stress is a crucial part in the design process [13].

The magnetic force generated in the SRM is reluctance type. Because the level of flux density at surfaces of the rotor and stator poles is high (when we have overlap between stator and rotor poles) stator and rotor poles experience a high value of electromagnetic surface forces during the commutation. The computation of the electromagnetic torque is based on the Maxwell Stress Tensor (MST) method. By using the MST method, the radial stress, τ_r, and tangential stress, τ_t, can be calculated as [14]:

$$\tau_t = \frac{1}{\mu_0} B_r B_t$$
$$\tau_r = \frac{1}{2\mu_0}(B_r^2 - B_t^2) \quad (1)$$

Here, B_r, B_t, and μ_0 are the radial flux density, tangential flux density, and vacuum permeability respectively. The tangential stress acting on the rotor poles generates torque. The radial stress acts in the radial direction of the stator pole and deforms the stator core, emitting noise. Since B_r is normally much larger than B_t, the radial force is one order of magnitude larger than the tangential force. Therefore, the radial force is the main electromagnetic source to generate vibration and noise [15, 16]. Figure 2 shows an example of the distribution of the magnetic surface force densities on the surface of the rotor poles. If we use the single phase excitation strategy to drive the motor, during each rotor stroke, the magnetic forces act on the four poles of the rotor.

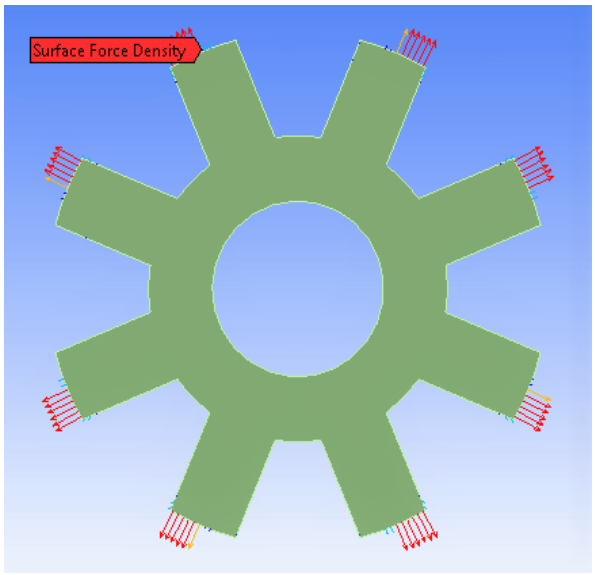

Figure 2. Imported surface force densities form ANSYS Maxwell to ANSYS Transient Structural

Results and Discussion

(a) Electromagnetic performance curves

The flux density distribution inside the rotor and stator cores for the aligned position of the rotor core is shown in Figure 3. The electric steel considered for the rotor and stator cores is *M270-35A*. As it is seen, the maximum value of flux density corresponding to the peak value of current is equal to 1.7Tesla.

Static characteristics of the motor are shown in Figures 4 and 5. Figure 4 shows the static torque versus the rotor position. As can be seen, the maximum value of the electric torque is equal to 14.3Nm which is a little bit higher than the rated torque of the motor. Figure 5 depicts the flux linkage for both aligned and unaligned positions of the rotor core. The rotor is optimized for minimum inductance in unaligned position.

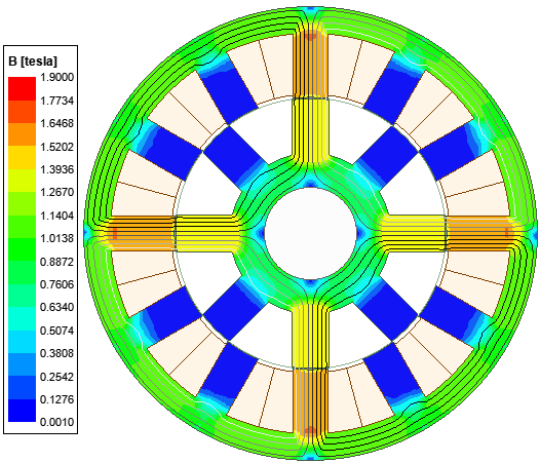

Figure 3. Flux density distribution due to excitation of one phase for the aligned position

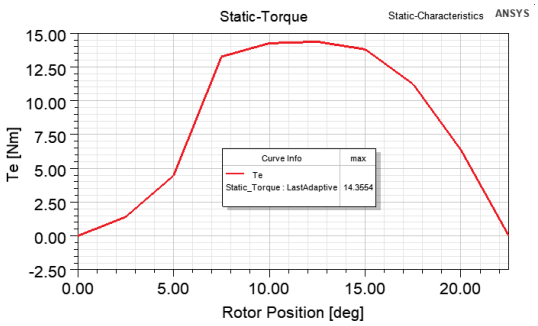

Figure 4. The static torque curve

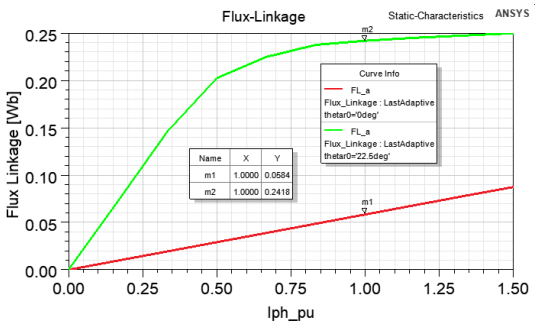

Figure 5. Flux linkage curves

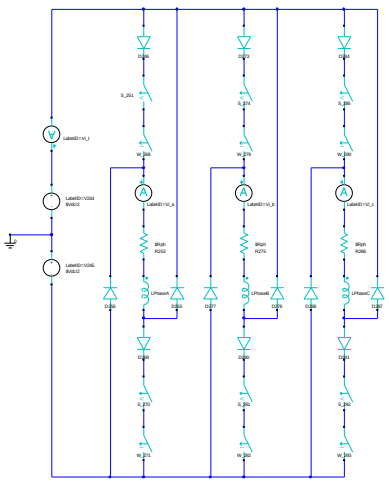

Figure 6. The drive circuit

For doing transient simulations, we considered the asymmetric bridge converter as shown in Figure 6. The values of on and off angles are set corresponding to maximum average torque for each rotor speed. Figure 7 shows the waveforms of the phase currents for the base speed. The peak value of the phase current is equal to 27A, and the RMS value is equal to 15.6A. Figure 8 depicts the phase flux linkages, and Figure 9 represents the electric torque for the base speed. Figure 10 shows the torque speed curve of the case-study motor.

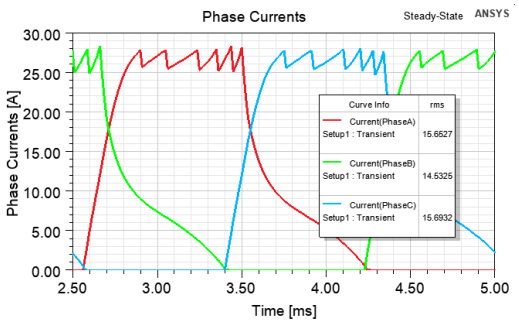

Figure 7. Phase currents for the base speed

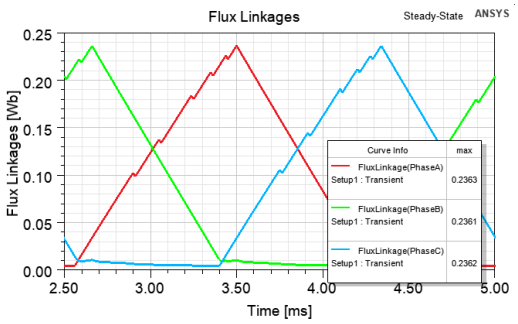

Figure 8. Phase flux linkages for the base speed

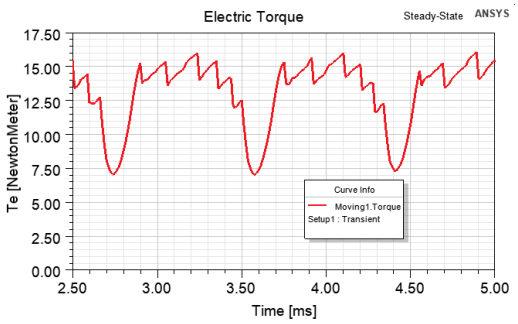

Figure 9. Electric torque for the base speed

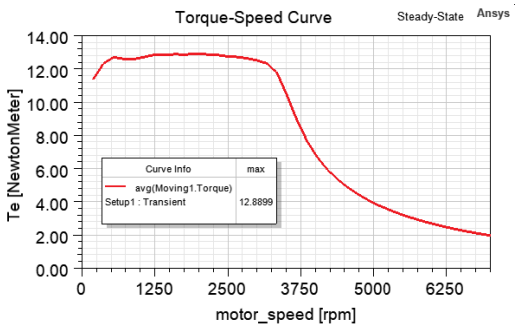

Figure 10. The torque-speed curve of the case study motor

(b) Structural analysis results

In this section, simulation results of the structural analysis of the motor for several rotor speeds are presented. Multi-physics simulations are performed in the ANSYS Workbench software. Surface force densities experienced by the rotor core are calculated by the ANSYS Maxwell software and imported to Transient Structural analysis. Both constant torque and constant power regions are considered**.** Figures 11 and 12 show the summary of results. The state of stress in the designed rotor is calculated using the von-Mises criterion. Figure 11 shows the maximum von-Mises stress over time for different rotor speeds. Also, the maximum deformation over time of the rotor geometry in both operating regions can be seen in Figure 12.

The grade of the electric steel of the stator and rotor cores is M270-35A. The Young's modulus of the material in the rolling direction is equal to 185GPa and in the transversal direction is equal to 200GPa. The tensile and yield strengths are equal to 565MPa and 450MPa respectively. If the stress that is experienced by the rotor is more than the yield strength of the material, it causes deformation and failure to the structure. According to Figure 11 and 12, the maximum von-Mises stress experienced by the rotor core is much lower than the yield strength which mean the rotor has a good rigidity for running at maximum speed. We know that the higher the speed, the greater the stress and deformation obtained. In both operating modes, the base speed and above base speed deformation are still less than 0.4mm air gap width (less than $5.9 \times 10^{-5} mm$ at base speed and less than $3.2 \times 10^{-4} mm$ at maximum speed).

The Figure 13 shows stress and deformation at several different operating speeds. Figure 13(a) and (b) shows stress and deformation in speed 1000rpm, Figure 13(c) and (d) in base speed 3000rpm, Figure 13(e) and (f) in speed 5000rpm and Figure 13(g) and (h) in maximum speed 7000rpm. Due to the robust structure of the rotor, the stresses and deformations experienced are very small, and the reliability of the motor will be maintained at the desired operating speeds.

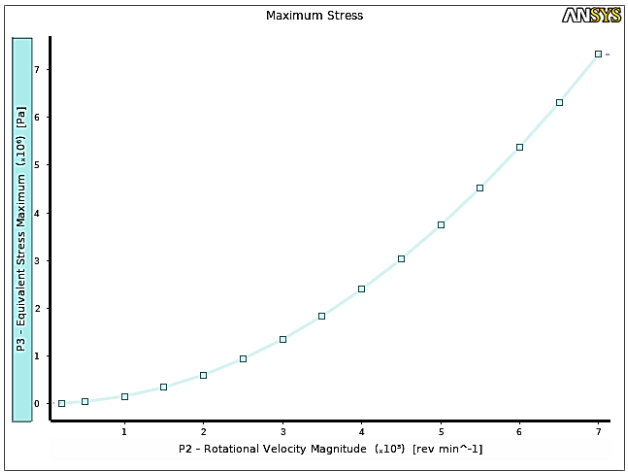

Figure 11. Maximum von-Mises stress over time as a function of the rotor speed

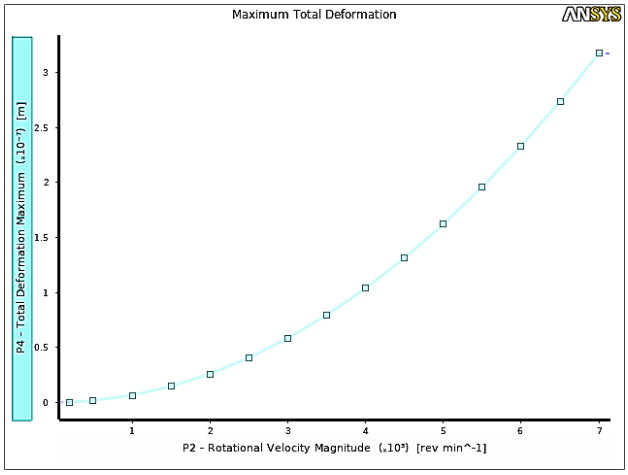

Figure 12. Maximum total deformation over time as a function of the rotor speed

As observed, the geometry of the rotor at the base speed experiences low stress and deformation, and the reliability of the motor is maintained. The experienced maximum stress is equal to $7.32 \times 10^{6} pa$ and lower than the yield strength of the rotor steel sheet**.** It is well known that centrifugal forces are the main cause of stress generation in objects with high rotation speed. As you can see, the stress and deformation at above base speed is more than the operating mode with base speed due to the dominance of centrifugal forces**.**

Conclusions

In this paper, a comprehensive analysis of the structural rigidity of a switched reluctance motor was presented. Deformations and stresses experienced by the rotor core are calculated by finite element method and presented. The aim was to calculate the stress experienced by the rotor for different operating speeds including both constant torque and constant power regions. The stress and deformation caused by magnetic force and centripetal force were obtained at the basic speed of 3000rpm and the maximum speed of 7000rpm. The mechanical stress in the rotor was compared with the yield strength of the material used in the rotor core. According to the obtained results, the maximum stress experienced by the rotor is less than the ultimate strength of the rotor material and does not exceed it. Therefore, the stress and deformation experienced does not cause structural failure and the reliability of the motor is maintained. The rotor core of SRM has significant structural strength in a wide range of speeds.

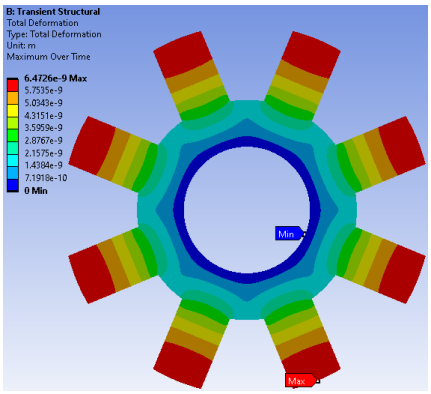

(a) 1000rpm

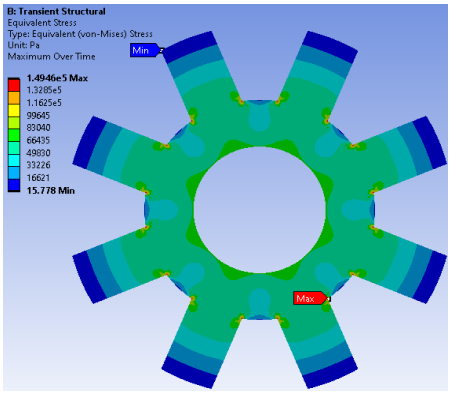

(b) 1000rpm

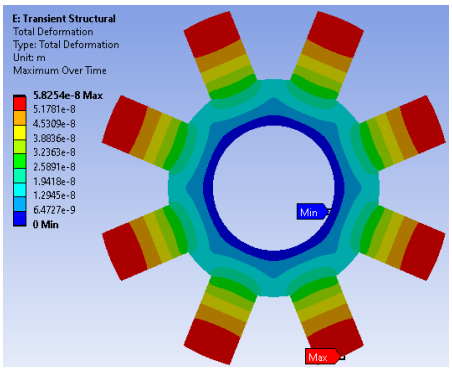

(c) 3000rpm

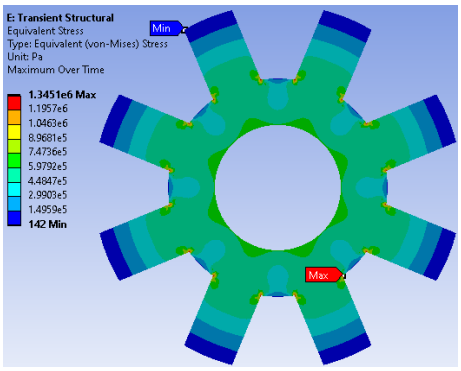

(d) 3000rpm

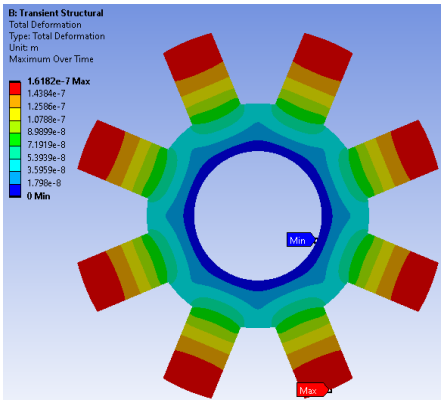

(e) 5000rpm

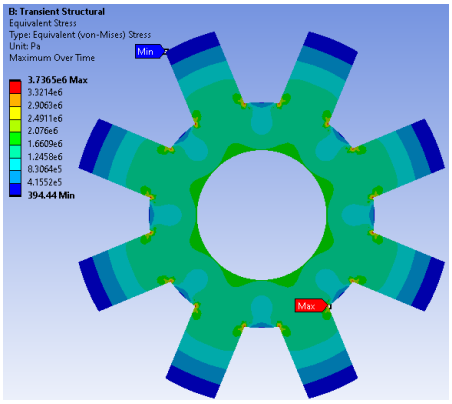

(f) 5000rpm

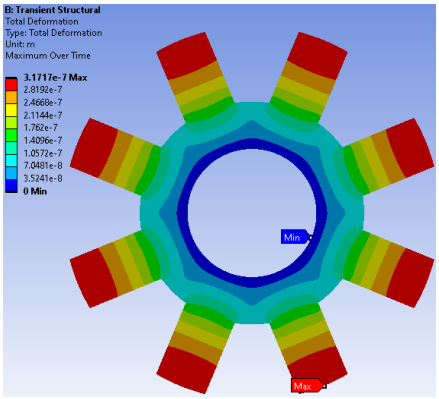

(g) 7000rpm

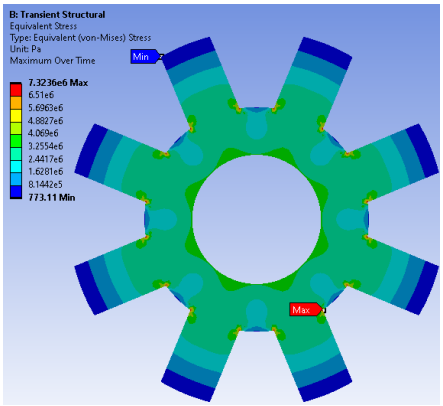

(h) 7000rpm

Figure 13. Simulation results for four different speeds, (a) (c) (e) (g): maximum total deformation over time, (b) (d) (f) (h): maximum von-Mises stress over time

References

[1] R. Krishnan, *Switched reluctance motor drives: modeling, simulation, analysis, design, and applications*. CRC press, 2017.

[2] B. Bilgin, J. W. Jiang, and A. Emadi, "Switched reluctance motor drives: fundamentals to applications," *Boca Raton, FL,* 2018.

[3] C. Pollock and C.-Y. Wu, "Acoustic noise cancellation techniques for switched reluctance drives," *IEEE transactions on industry applications,* vol. 33, no. 2, pp. 477-484, 1997.

[4] I. Husain, "Minimization of torque ripple in SRM drives," *IEEE transactions on Industrial Electronics,* vol. 49, no. 1, pp. 28-39, 2002.

[5] G. Liu, G. Qiu, F. Zhang, F. Qiu, and W. Cao, "Outer rotor mechanical and dynamic performance analysis for high-speed machine," in *2016 IEEE Transportation Electrification Conference and Expo, Asia-Pacific (ITEC Asia-Pacific)*, 2016, pp. 509-513: IEEE.

[6] M. Besharati, K. Pullen, J. Widmer, G. Atkinson, and V. Pickert, "Investigation of the mechanical constraints on the design of a super-high-speed switched reluctance motor for automotive traction," 2014.

[7] C. Monissen, M. E. Arslan, A. Krings, and J. Andert, "Mechanical Stress in Rotors of Permanent Magnet Machines—Comparison of Different Determination Methods," *Energies,* vol. 15, no. 23, p. 9169, 2022.

[8] K. Yamazaki and A. Aoki, "3-D electromagnetic field analysis combined with mechanical stress analysis for interior permanent magnet synchronous motors," *IEEE Transactions on Magnetics,* vol. 52, no. 3, pp. 1-4, 2015.

[9] P. Rasilo *et al.*, "Modeling of hysteresis losses in ferromagnetic laminations under mechanical stress," *IEEE Transactions on Magnetics,* vol. 52, no. 3, pp. 1-4, 2015.

[10] L. Maharjan, S. Wang, A. H. Isfahani, W. Wang, and B. Fahimi, "Comparative study of structural rigidity of induction machine and switched reluctance machine," in *2014 IEEE Transportation Electrification Conference and Expo (ITEC)*, 2014, pp. 1-5: IEEE.

[11] J. Li, X. Song, and Y. Cho, "Comparison of 12/8 and 6/4 switched reluctance motor: Noise and vibration aspects," *IEEE transactions on magnetics,* vol. 44, no. 11, pp. 4131-4134, 2008.

[12] A. A. Dedkova, P. Y. Glagolev, G. D. Demin, E. E. Gusev, and P. A. Skvortsov, "Mechanical Stresses Analysis of Thin Round Membranes in the Case of Large Deflections," in *2020 IEEE Conference of Russian Young Researchers in Electrical and Electronic Engineering (EIConRus)*, 2020, pp. 2288-2292: IEEE.

[13] M. E. Gerlach, M. Zajonc, and B. Ponick, "Mechanical stress and deformation in the rotors of a high-speed PMSM and IM," *e & i Elektrotechnik und Informationstechnik,* vol. 138, no. 2, pp. 96-109, 2021.

[14] G. Fang, J. Ye, D. Xiao, Z. Xia, and A. Emadi, "Lumped Radial Force Characteristics Reconstruction for Switched Reluctance Machines through Scaling Flux-linkage Characteristics," *IEEE Transactions on Magnetics,* 2022.

[15] G. Fang, F. P. Scalcon, D. Xiao, R. P. Vieira, H. A. Gründling, and A. Emadi, "Advanced control of switched reluctance motors (SRMs): A review on current regulation, torque control and vibration suppression," *IEEE Open Journal of the Industrial Electronics Society,* vol. 2, pp. 280-301, 2021.

[16] A. Tanabe and K. Akatsu, "Vibration reduction method in SRM with a smoothing voltage commutation by PWM," in *2015 9th International Conference on Power Electronics and ECCE Asia (ICPE-ECCE Asia)*, 2015, pp. 600-604: IEEE.